Supporting Information

Materials and Chemicals. Asialofetuin from fetal calf serum (ASF) and myoglobin from horse heart (MYO), dithiothreitol (DTT), acetonitrile (ACN), ammonium bicarbonate (NH_4HCO_3), urea, MALDI matrix (α-cyano-4-hydroxycinna mic acid, CHCA), and trifluoroacetic acid (TFA) were obtained from Sigma-Aldrich. Sequencing grade modified trypsin was from Promega. The glyceol free peptide-N-glycosidase (PNGase F, 500 units/μL) was from New England Biolabs. Sep-Pak C18 columns were from Waters. Human serum were provided by Fudan University Shanghai cancer center and stored at – 80 °C before analysis. Ammonia, $FeCl_3 \cdot 6H_2O$, ammonium acetate (NH_4Ac), sodium citrate, ethylene glycol, and tetraethyl orthosilicate (TEOS) were obtained from Sinoreagent Chemical Reagent Co. Ltd. 1-(3-Dimethylaminopropyl)-3-ethylcarbodiimide (EDC) , and p-nitrobenzoic acid were obtained from Aladdin Chemical Reagent Co.,Ltd. Other chemical reagents were of analytical grade and obtained from Shanghai Chemical Reagent Co., Ltd., which were used as received without further puri fication. The water used in the experiments was ultrapure water obtained from a Milli-Q Water System (Millipore, Bedford, MA).

Preparation of Fe_3O_4 nanoparticles: The Fe_3O_4 nanoparticles were prepared through a modified solvothermal reaction. Typically, 1.35 g of $FeCl_3 \cdot 6H_2O$, 3.85 g of NH_4Ac, and 0.40 g of sodium citrate were dissolved in 70 mL of ethylene glycol. The mixture were stirred vigorously for 1 h at 170 ^oC to form a homogeneous black solution and then transferred into a Teflon-lined stainless-steel autoclave (100 mL capacity). The autoclave was heated at 210 ^oC and maintained for 18 h; then it was cooled to room temperature. The black product was washed twice with ethanol and collected with the help of a magnet, and finally dried in the vacuum oven overnight at 40 ^oC.

Preparation of Fe_3O_4 @SiO_2 core-shell nanoparticles: The Fe_3O_4@SiO_2 core-shell nanoparticles were prepared through a modified stober method. Typically, Fe_3O_4 nanoparticles (0.10 g) were dispersed in ethanol (80 mL) with 0.5 h sonication followed by a sequential addition of ammonia (25%, 1.00 mL), water (20.0 mL), and TEOS (1.0 mL), the resulting mixture was

stirred for 12 h at room temperature. The product was washed several times with ethanol and water with the help of a magnet. The final product was dispersed in iso-propanol for further use.

Synthesis of nitrobenzol silane coupling agents (NBTES): (3-aminopropyl)triethoxysilane (884 mg, 4.00 mmol), p-nitrobenzoic acid (668 mg, 4.00 mmol), EDC (958mg, 5.00 mmol) and ACN (80 mL) were taken in 150 mL round bottom flask and stirred at room temperature over night. The mixture was concentrated under reduced pressure and was dissolved in 50 mL ethyl acetate. The solvent was washed by 50 mL 1M $KHSO_4$ aqueous solution and 50 mL 1 M $NaHCO_3$ aqueous solution. The oil phase was concentrated under reduced and purified by flash chromatography on silica gel using ethyl acetate to afford pure NBTES as pale yellow solid (952 mg, 64.3%):1H NMR(400MHz,d6-DMSO):δ 8.80(s, 1H), 8.31(d, 2H), 8.07(d, 2H), 3.75(q, 2H), 1.59(m, 2H),1.15(t, 9H), 0.60(t. 2H);13C NMR:164.52(NHCO), 148.91(NO_2C), 140.41(COC), 128.66(CH), 123.49(CH), 56.10(CH2), 42.57(CH2), 23.51(CH2), 18.56(CH3), 11.39(CH2);

Preparation of Fe_3O_4@SiO_2-Aniline nanoparticles: The Fe_3O_4@SiO_2-Aniline nanoparticles were prepared by modified the Fe_3O_4@SiO_2 nanoparticles with NBTES and then reduced by zinc powder, briefly. 200 mg Fe_3O_4@SiO_2 was dispersed in 60 mL of isopropanol, and then 50 mg NBTES was added into the suspension. After the reaction solution was mechanically stirred for 24 h, the Fe_3O_4@SiO_2-Nitrobenzol was collected by magnetic separation and dispersed in 60 mL saturated NH_4Cl aqueous solution with 10% DMF. Then, 100 mg Zinc powder was added into the dispersion solvent. After 1 hour mechanical stirring, the products were collected by magnetic separation and washed with ethanol and water, finally dried in the vacuum oven overnight at 40 ^oC for further use. It was documented that the yield of reduction of nitro group to aniline with Zinc powder in NH_4Cl aqueous solution were almost above 84% [T. Takehito, T, Hirohisa, Green Chem., 2001, 3, 37–38]. This is the reason that we chose the present synthesis method.

Enrichment of N-glycoproteome with Fe_3O_4@SiO_2-Aniline nanoparticles and nano1DLC-MS/MS analysis: The serum was thawed on wet ice, and 1 μL of serum sample was diluted with 20 μL denaturing solution which contained 60 mM NH_4HCO_3 and 8 M urea. The mixture was treated with 10 mM dithiothreitol (DTT) at 57° C for 30 min and alkylated with 20 mM

iodoacetamide (IAA) at room temperature for 1 h in the dark. Prior to digestion, the solution was diluted with 25 mM NH_4HCO_3 until the final concentration of urea was less than 1.5 M. Trypsin was added according to the enzyme-to-substrate ratio of 1:30 (w/w) and hydrolyzed for 16 h under gentle shaking. The digests were desalted by C_{18} columns and the eluted peptides were lyophilized for further use. The lyophilized serum sample was redissolved in oxidation buffer (pH=5.5) containing 100 mM sodium acetate and 150 mM NaCl. Then the cis-diols of carbohydrate groups on the glycopeptides were oxidized by 10 mM sodium periodate ($NaIO_4$) at room temperature for 1 h in the dark under constant shaking, followed by the use of 20 mM sodium sulfite to quench the oxidation through incubating for another 10 min at room temperature. The oxidized samples were lyophilized and and resuspended in the coupling solution. The Aniline-functional nanoparticles which had been prewashed twice with the coupling solution (70% methanol and 30% acetic acid (v/v)) was added with the mass ratio of protein: Fe3O4@SiO2-Aniline of 1:1 and incubated at 60 ^oC for 4 h under constant shaking and then a magnetic was used to collect the Fe_3O_4@SiO_2-Aniline nanoparticles. The mass ratio of protein: Fe3O4@SiO2-Aniline was optimized and determined using standard protein mixutres using the following method. To determine the mass ratio of Fe_3O_4@SiO_2-Aniline nanoparticles to protein digests, different amounts of mass ratio of Fe_3O_4@SiO_2-Aniline nanoparticles were used to enrich glycopeptides from asialofetuin digests. In detail, 1 mg of the digest was enriched with different amounts Fe_3O_4@SiO_2-Aniline nanoparticles (0.2，1, 5 and 10 mg) under the optimized temperature, solvent and et al. Each sample solution after glycopeptide enrichment was spotted onto six different wells on a MALDI plate. The mean relative intensities of a representative deglycopeptides m/z 3017 were plotted against the addition amounts of Fe_3O_4@SiO_2-Aniline. The mass ratio of protein digests to Fe_3O_4@SiO_2-Aniline is approximatlly 1 mg protein/per mg Fe_3O_4@SiO_2-Aniline (Figure S7). Then, the nanoparticles were washed with washing buffers sequentially. Afterward, the deglycosylated peptides were released through incubation the nanoparticle with 50 mM NH_4HCO_3 containing 1 μL of PNGase F (500 units per μL) at 37 ^oC overnight. The supernatant containing the released deglyosylated peptides was collected through magnet separation and lyophilized for nano-LC MS/MS analysis. The nano-LC MS/MS analysis was performed on a LC-20AD system (Shimadzu, Tokyo, Japan) connected to a LTQ orbitrap mass spectrometer (Thermo Electron, Bremen, Germ any) equipped with an online nanoelectrospray ion source (Michrom Bioresources, Auburn, CA).The lyophilized

sample was resuspended with 5% ACN containing 0.1% FA. Then the sample solution was injected into a CAPTRAP column (0.5 × 2 mm, MICHROM Bioresources, Auburn, CA) in 4 min with a flow rate of 20 μL/min. Subsequently, a linear gradient of acetonitrile of from 5 to 45% (95% ACN in 1% FA) over 100 min at a flow rate of 500 nL/min was applied. The separated samples were introduced into the mass spectrometer via an ADVANCE 30 μm silica tip (MICHROM Bioresources, Auburn CA). The spray voltage was set at 1.6 kV, and the capillary was heated to 180 °C. The mass spectrometer was operated in a data-dependent mode. For each cycle of duty, it consisted of one full-MS survey scan at the mass range of 400 −2000 Da with a resolution power of 100000. Then MS/MS scan was conducted for eight of the most abundant precursor ions by LTQ section with a dynamic exclusion duration of 90 s. Only peaks with the charge of 2+ and 3+ could be selected for the MS/MS run. The AGC expectation during full MS and MS/MS were 1×10^6 and 10000, respectively. All tandem mass spectra were collected through the LTQ section using collision-induced dissociation with helium as the collision gas and a normalized collision energy value set as 35.0%. The system control and data collection were achieved through Xcalibur, version 1.4 (Thermo).

Data analysis: The data derived from the ESI MS/MS analysis was searched by SEQUEST, against a composite database, including both original and reversed human protein database of international protein index (Combine.human.uniprot.sprot.090210.fasta).The relevant parameters were set to the following modifications: enzyme was selected as trypsin (partially enzymatic). A maximum of two missed cleavages (MCs) was allowed. Carboxamidomethylation (C, 57.02150) was set as a fixed modification and the oxidation (M, 15.99492) as well as asparagine deglycosylation (N, 0.98402) were set as variable modifications. Precursor mass and fragment mass tolerance were 10 ppm and ±0.6 Da for the SEQUEST search. Mass value was set as monoisotopic. To statistically validate the accuracy of peptide assignments to tandem mass spectra from SEQUEST, Trans-Proteomic Pipeline (TPP) was applied to effectively compute the probability for the likelihood of each identification being correct in a data-dependent fashion. Only those peptides that passed the peptide probability threshold 0.95 were accepted for further data interpretation. The Asn modification that did not occur in the N-X-S/T motif (X≠P) was eliminated to ensure the false positive rate below 1% for the identified glycosylation sites.

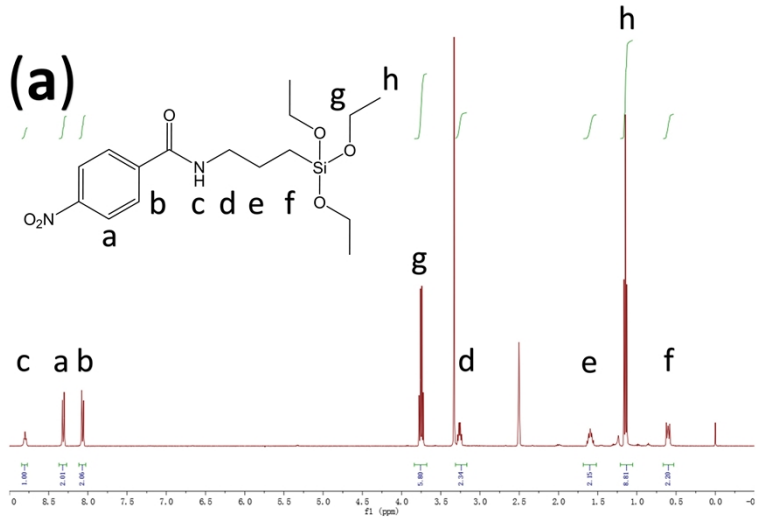

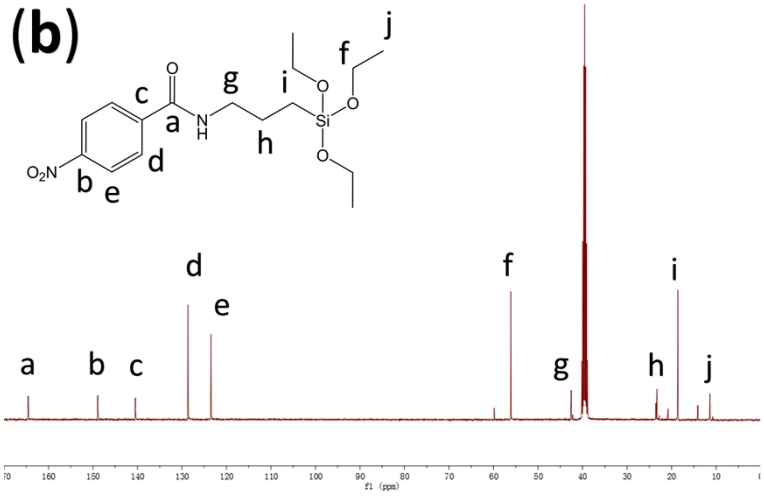

Figure S1 H^1 NMR and (b) C^{13} NMR spectra of the nitrobenzol functionalized silane coupling agent (NBTES).

Table S1 ZETA potential of Fe_3O_4@SiO_2, Fe_3O_4@SiO_2-Nitrobenzol and Fe_3O_4@SiO_2-Aniline.

	ZETA Potential
Fe_3O_4@SiO_2	-20.4 mV
Fe_3O_4@SiO_2-Nitrobenzol	-16.3 mV
Fe_3O_4@SiO_2-Aniline	+ 6.3 mV

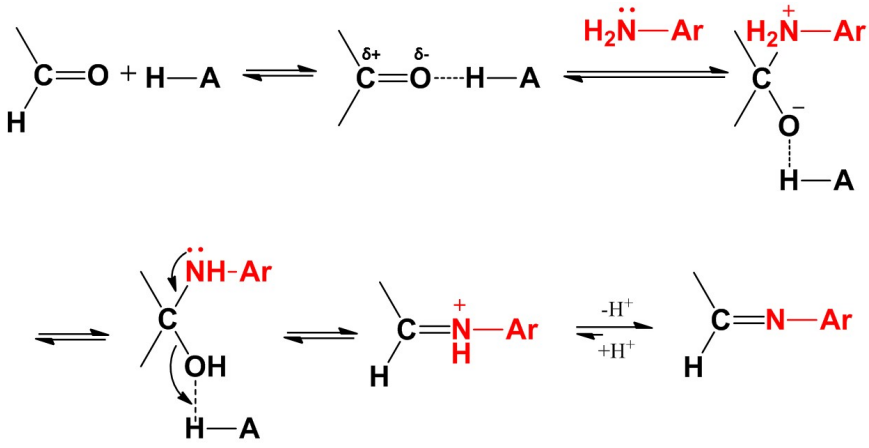

Figure S2 Proposed main reaction pathways of the nonreductive amination reaction. Generally, carbonyl groups would combine acid molecules via Hydrogen bonds under weakly acidic conditions, and this led to the enhancement of carbonyl groups' electrophilicity. Then, the amino groups attack the carbonyl groups. After the proton transfer and dehydration processes, the imine bonds found as it was shown.

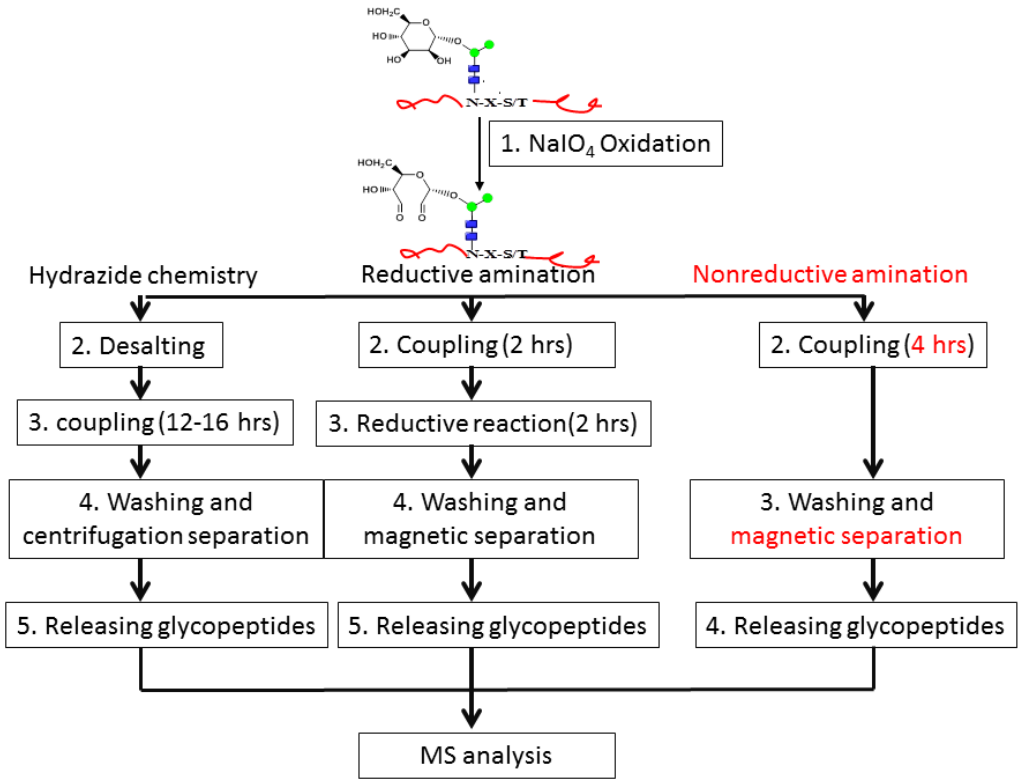

Figure S3 The enrichment procedure of hydrazide chemistry-based method, reductive amination-based method and nonreductive amination-based method.

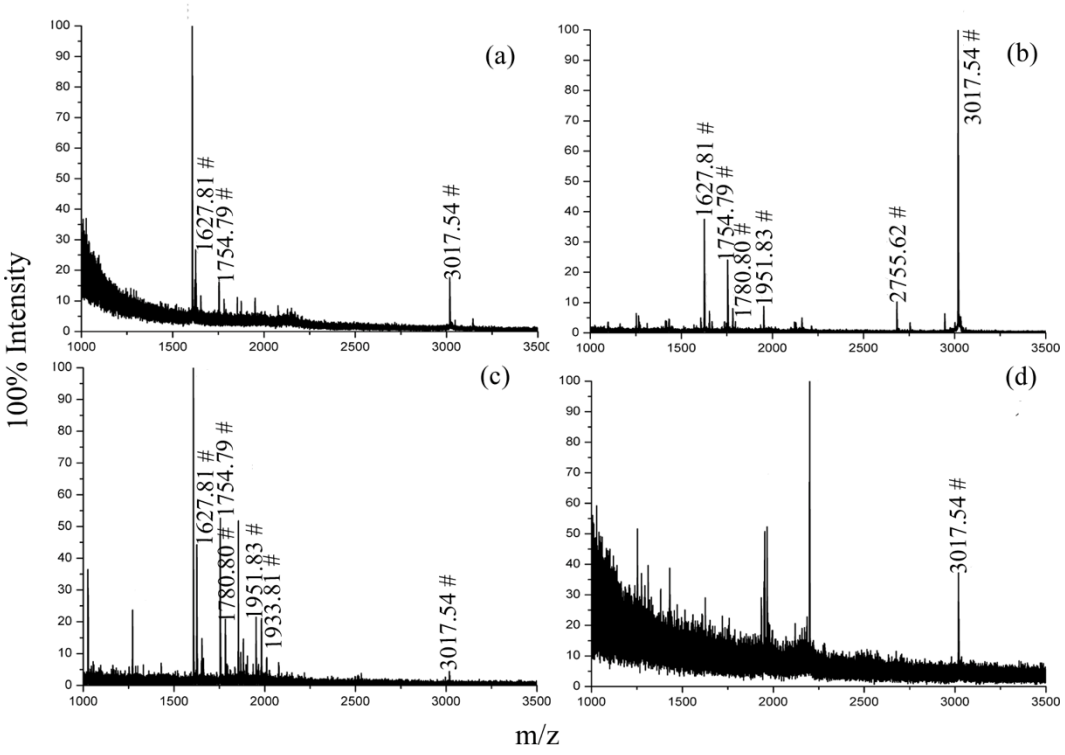

Figure S4 MALDI-TOF mass spectra of tryptic digest mixture of asialofetuin (with a mole ratio of ASF: MYO=1:1) after enrichment using Fe_3O_4@SiO_2-Aniline and delycosylation by PNGase F. The enrichment was perforemed in different coupling buffer (a) 50% ACN with 1% TFA, (b) 70% methanol and 30% acetic acid (v/v), (c) 70% ACN and 30% acetic acid (v/v) and (d) NH_4Ac aqueous (pH 2.0) . "#" represent the deglycosylated glycopeptides.

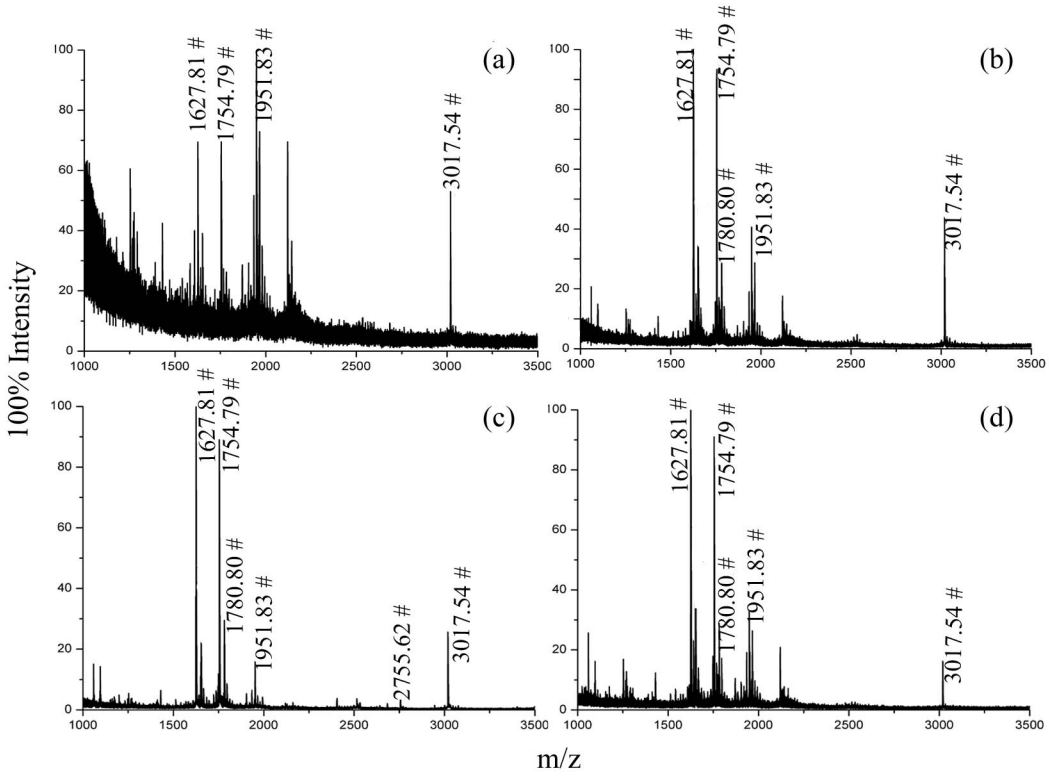

Figure S5 MALDI-TOF mass spectra of tryptic digest mixture of asialofetuin and myoglobin (with a mole ratio of ASF: MYO=1:1) after enrichment using Fe_3O_4@SiO_2-Aniline and delycosylation by PNGase F. The enrichment was performed with different coupling time (a) 30 min, (b) 2 h, (c) 4 h and (d) 8 h. "#" represent the deglycosylated glycopeptides.

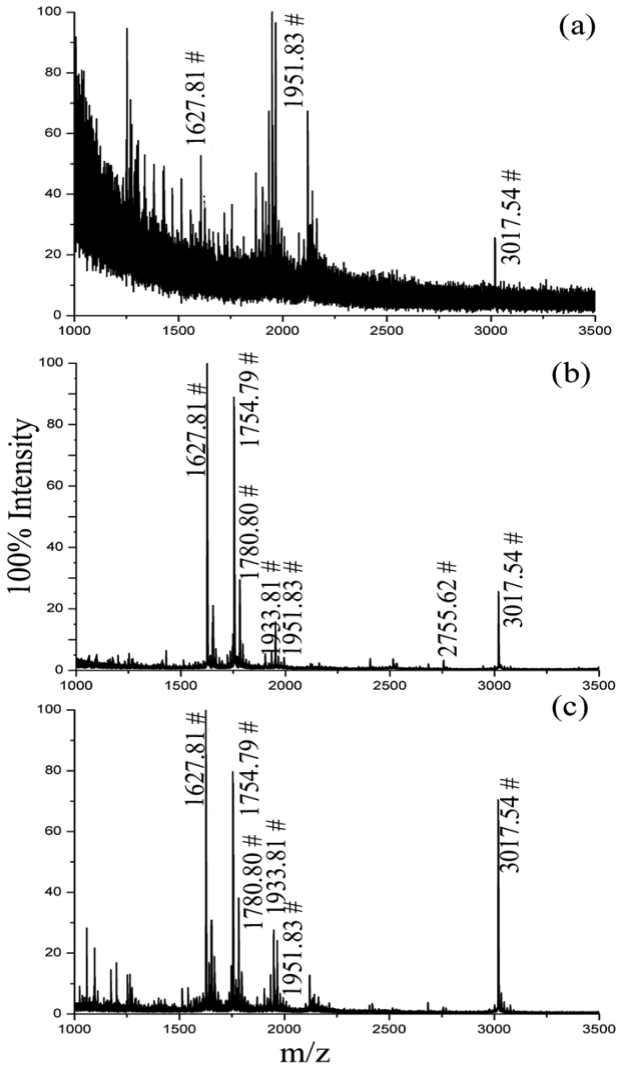

Figure S6 MALDI-TOF mass spectra of tryptic digest mixture of asialofetuin and myoglobin (with a mole ratio of ASF: MYO=1:1) after enrichment using Fe_3O_4@SiO_2-Aniline and delycosylation by PNGase F. The enrichemnt was performed under different coupling temperature (a) 37 ^oC, (b) 60 ^oC and (c) 75 ^oC. "#" represent the deglycosylated glycopeptides.

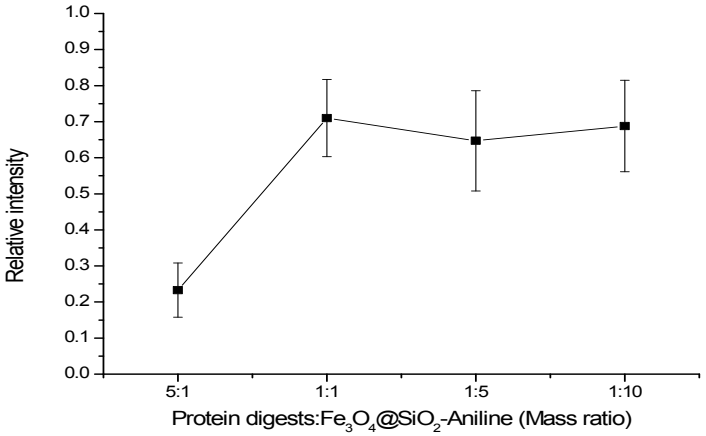

Figure S7 Influence of the Fe_3O_4@SiO_2-Aniline amounts on the enrichment of glycopeptides from the asialofetuin digests.

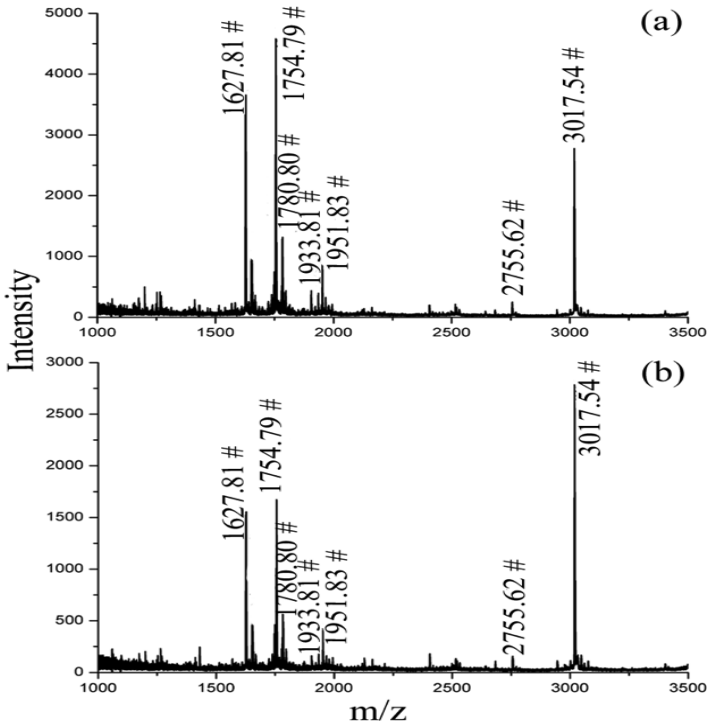

Figure S8 MALDI-TOF mass spectra of tryptic digest mixture of asialofetuin and myoglobin (with a mole ratio of ASF: MYO=1:1) after enrichment using Fe_3O_4@SiO_2-Aniline and delycosylation by PNGase F. The enrichment was performed (a) without and (b) with the addition of a reductive reagent during the coupling process. "#" represent the deglycosylated glycopeptides.

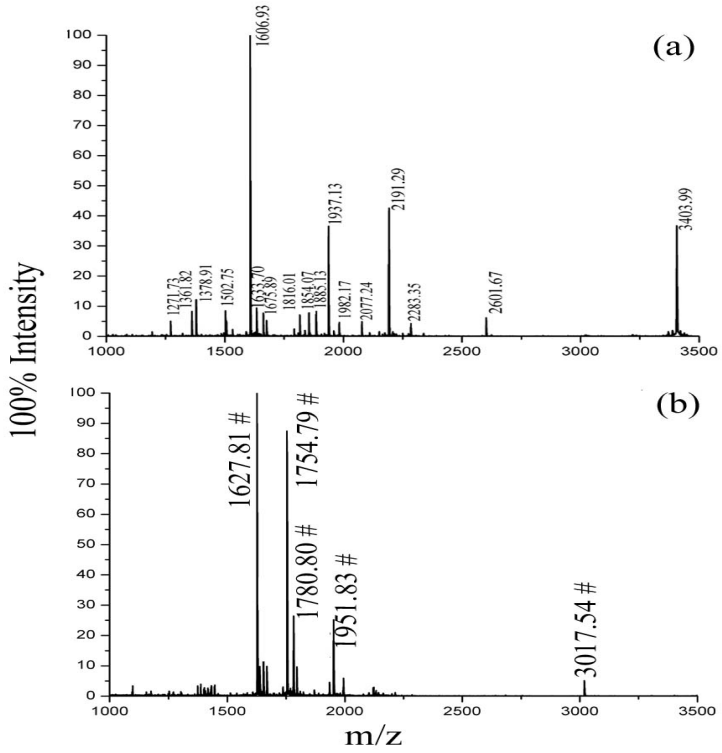

Figure S9 MALDI-TOF mass spectra of tryptic digest mixture of asialofetuin and myoglobin (with a molar ratio of ASF: MYO=1:100) (a) direct analysis (b) analysis after isolation by Fe_3O_4@SiO_2-Aniline and deglycosylation by PNGase F. "#" represent the deglycosylated glycopeptides.

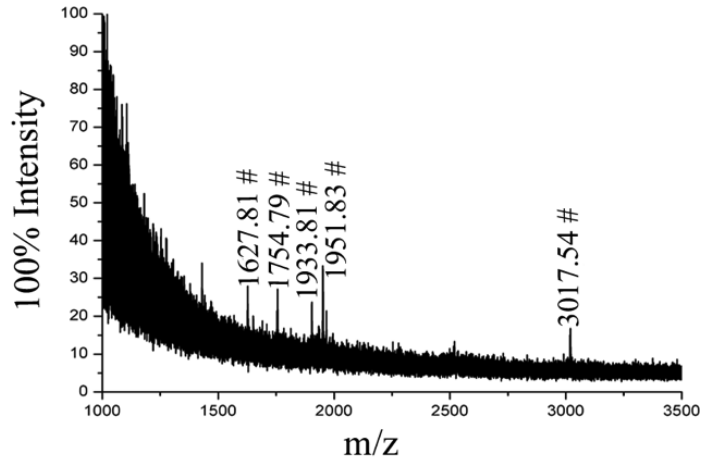

Figure S10 MALDI-TOF mass spectra of tryptic digest of asialofetuin after isolation by Fe_3O_4@SiO_2-Aniline and deglycosylation by PNGase F. The initial concentration of asialofetuin digests is 5.0 ng/μL. "#" represent the deglycosylated glycopeptides.

Table S2 List of identified glycoproteins from 1 μL human serum after solid phase extraction with Fe_3O_4@SiO_2-Aniline, N# denotes the N-linked glycosylation site.

No	Protein	Description	Peptide Sequence
1	P01024|AACT_HUMAN	Complement C3	TVLTPATNHMGN#VTFTIPANR
2	P02768|ALBU_HUMAN	Serum albumin	CTAFHDN#ETFLK EFN#ETFTFHADICTLSEK LVN#VTEFAK YICEN#DSISSK
3	P01009|A1AT_HUMAN	Alpha-1-antitrypsin	YLGN#ATAIFFLPDEGK QLAHQSN#STNIFFSK EGLNFN#LTEIPEAQIHEGFQELLR
4	P02787|TRFE_HUMAN	Haptoglobin	R.QQQHLFGSN#VTDCSGNFCK AVAN#FSGSCAPCA QQQHLFGSN#VTDCSGNF CGLVPVLAENYN#KSDNCE
5	P00450|CERU_HUMAN	Ceruloplasmin	EHEGAIYPDN#TTDFQR EN#LTAPGSDSAVFFEQGTTR MLLATEEQSPGEGDGN#VTR NN#GTYYSPNYNPQSR SVVDEN#FSWYLEDNIK ELHHLQEQN#VSNAFLDK
6	P01023|A2MG_HUMAN	Alpha-2-macroglobulin	SIN#TTNVMGTSLTVR ETTFN#STLLCPSGGEVSEELSLK FSGQLN#STHGCFYQQVK HNVYIN#GTYTPVSSTNEK SLGNVN#FTVSAEALESQELCGTEV PSVPEHGR VSN#QTLSLFF NEANYYSN#ATTDEHGLVQF YILN#GTLLGLK
7	P04114|APOB_HUMAN	Apolipoprotein B-100	R.FN#SSYLQGTNQITGR.Y QVLFLDTVYGN#CSTHF

8	P10909|CLUS_HUMAN	Clusterin	KKEDALN#ETR LAN#LTQGEDQYYLR QLEEFLN#QSSPF MLN#TSSLLEQLNEQF
9	P0C0L4|CO4A_HUMAN	Complement C4-A	GLN#VTLSSTGR. FSDGLESN#SSTQFEVK GLN#VTLSSTGR LVN#GSHISLSK
10	P01011|AACT_HUMAN	Alpha-1-antichymotrypsin	HPNSPLDEEN#LTQENQDR FN#LTETSEAEIHQSF NSPLDEEN#LTQENQDR AFLSLGAHN#TTLTEILK TLN#QSSDELQLSMGNAMFVK
11	P00738|HPT_HUMAN	Haptoglobin	NLFLN#HSEN#ATAK SPVGVQPILN#HTF VVLHPN#YSQVDIGLIK MVSHHN#LTTGATLINEQWLLTTAK VDSGN#DTDIADDGCPKPPEIAHGY VEHSVR
12	P01857|IGHG1_HUMAN	Ig gamma-1 chain C region	EEQYN#STYR SCSVMHEALHN#HTQK N#VSLTCLVK
13	Q14624|ITIH4_HUMAN	Inter-alpha-trypsin inhibitor heavy chain H4	LPTQN#ITFQTESSVAEQEAEFQSPK
14	P19827||ITIH1_HUMAN	Inter-alpha-trypsin inhibitor heavy chain H1	AN#LSSQALQMSLDYGFVTPL
15	P02765|FETUA_HUMAN	Alpha-2-HS-glycoprotein	KVCQDCPLLAPLN#DTR AALAAFNAQNN#GSNFQLEEISR
16	P02766|TTHY_HUMAN	Transthyretin	EVVFTAN#DSGPR

17	P01876|IGHA1_HUMAN	Ig alpha-1 chain region	LAGKPTHVN#VSVVMAEVDGTCY
18	P04004|VTNC_HUMAN	Vitronectin	N#ISDGFDGIPDNVDAALALPAHSYNN#ATVHEQVGGPSLTSDLQAQSK
19	P01871|IGHM_HUMAN	Ig mu chain C region	YKN#NSDISSTR THTN#ISESHPN#ATF GLTFQQN#ASSMCVPDQDTAIR STGKPTLYN#VSLVMS
20	P02774|VTDB_HUMAN	Vitamin D-binding protein	LCDN#LSTK
21	P01859|IGHG2_HUMAN	Ig gamma-2 chain C region	EEQFN#STFR SLSSVVTVPSSN#FTQTYTCNVDHKPSNTK
22	P11464|	Pregnancy-specific beta-1-glycoprotein 1	ETAYSN#ASLLIQN#VTR
23	P11465	Pregnancy-specific beta-1-glycoprotein 2	ETAYSN#ASLLIQN#VTR
24	P04196|HRG_HUMAN	Histidine-rich glycoprotein	HSHNN＃NSSDLHPHK VIDFN#CTTSSVSSALANTK
25	P01042||KNG1_HUMAN	Kininogen-1	SIVQTN#CSK
26	P36955|PEDF_HUMAN	epithelium-derived factor Haptoglobin	VTQN#LTLIEESLTSEFIHDIDR
27	P01008|ANT3_H	Antithrombin-III	WVSN#KTEGR LGACN#DTLQQLMEVFK

	UMAN		N#ETYQDISELVYGAK ITDVIPSEAIN#ETVL
28	P08185|CBG_HUMAN	Corticosteroid-binding globulin	AQLLQGLGFN#LTER
29	Q08380|LG3BP_HUMAN	Galectin-3-binding protein	TVIRPFYLTN#SSGVD
30	P02763|A1AG1_HUMAN	Alpha-1-acid glycoprotein 1	QDQCIYN#TTYLNVQR YFTPN#KTEDTIFLR LVPVPITN#ATLDQITGK CANLVPVPITN#ATLDQITGK
31	P00734|THRB_HUMAN	Prothrombin	GHVN#ITR SEGSSVN#LSPPLEQCVPDR
32	P00739|HPTR_HUMAN	Haptoglobin-related protein	NLFLN#HSEN#ATAK
33	P27169|PON1_HUMAN	Serum paraoxonase/arylesterase 1	VTQVYAEN#GTVLQGSTVASVYK VAEGFDFANGIN#ISPDGK
34	P25311|ZA2G_HUMAN	Zinc-alpha-2-glycoprotein	DIVEYYNDSN#GSHVLQGR
35	P43652|AFAM_HUMAN	Afamin	DIENFN#STQK AESPEVCFN#ESPK
36	P13645	Keratin, type I cytoskeletal 10	NQILN#LTTDNANILLQIDNAR N#VSTGDVNVEMNAAPGVDLTQLLNNMR TIDDLKNQILN#LTTDNANILLQIDNAR
37	P35527	Keratin, type I cytoskeletal 9	N#YSPYYNTIDDLKDQIVDLTVGNNK

38	P20742	Pregnancy zone protein	TFSSMTCASGAN#VSEQLSLKLPSN VVK
39	P05787	Keratin, type II cytoskeletal 8	LESGMQN#MSIHTK
40	P02750	Leucine-rich alpha-2-glycoprotein	DKMFSQN#DTR
41	P13647	Keratin, type II cytoskeletal 5	AQYEEIAN#RSR
42	P01616	Ig kappa chain V-II region MIL	FSGSGSGTN#FTLK
43	P15924	Desmoplakin	AN#SSATETINK
44	P35659	Protein DEK	KNQN#SSKK
45	P23471	Receptor-type tyrosine-protein phosphatase zeta	N#FTLRNTK CN#MSSDGSEHSLEGQK
46	P05155|IC1_HUMAN	Plasma protease C1 inhibitor	TN#LSILSYPK VGQLQLSHN#LSLVILVPQNLK VLSN#NSDANLELINTW
47	P05090|APOD_HUMAN	Apolipoprotein D	ADGTVNQIEGEATPVN#LTEPAK N#ITSNNIDVK
48	P02748|CO9_HUMAN	Complement component C9	AVN#ITSENLIDDVVSLIR
49	P02749|APOH_HUMAN	Beta-2-glycoprotein 1	VYKPSAGN#NSLYR FICPLTGLWPIN#STLK LGN#WSAMPSCK DTAVFECLPQHAMFGN#DTITCTTH GN#WTK
50	P02745|C1QA_HUMAN	Complement C1q subcomponent subunit A	NQEEPYQN#HSGR

51	P02751|FINC_HUMAN	Fibronectin	LDAPTNLQFVN#ETDSTVLVR
52	P02790|HEMO_HUMAN	Hemopexin	N#GTGHGN#STHHGPEYMR ALPQPQN#VTSLLGCTH SWPAVGN#CSSALR
53	P03952|KLKB1_HUMAN	Plasma kallikrein	LQAPLN#YTEFQKPICLPSK IYPGVDFGGEELN#VTFVK
54	P04003|C4BPA_HUMAN	C4b-binding protein alpha chain	FSLLGHASISCTVEN#ETIGVWRPSP PTCEK
55	P04217|A1BG_HUMAN	Alpha-1B-glycoprotein	FQSPAGTEALFELHN#ISVA LHDNQN#GSGDSAPVELILS
56	P04220|MUCB_HUMAN	Ig mu heavy chain disease protein	THTN#ISESHPN#ATF
57	P04278|LUM_HUMAN	Sex hormone-binding globulin	THSCPQSPGN＃GTDASH
58	P51884||IC1_HUMAN	Lumican	AFEN#VTDLQWLILDHNLLENSK LGSFEGLVN#LTF
59	P05546|HEP2_HUMAN	Heparin cofactor 2	N#LSMPLLPADFHK
60	P07996|TSP1_HUMAN	Thrombospondin-1	VVN#STTGPGEHLR
61	P0C0L5|CO4B_HUMAN	Complement C4-B	GLN#VTLSSTGR
62	P08603|C	Complement	MDGASN#VTCINSR

	FAH_HUMAN	factor H	AQTTVTCMEN#WSPTPR ISEEN#ETTCYMGK SPDVIN#GSPISQK IPCSQPPQIEHGTIN#SSR
63	P19652|A1AG2_HUMAN	Alpha-1-acid glycoprotein 2	QNQCFYN# SSYLNVQR YFTPN#KTEDTIFLR
64	P19823|ITIH2_HUMAN	Inter-alpha-trypsin inhibitor heavy chain H2	VVN#NSPQPQNVVFDVQIPK GAFISN#FSMTVDGK
65	P25090|FPR2_HUMAN	N-formyl peptide receptor 2	ETN#FSTPLNEYEEVSYESAGYTVLR
66	P29622|KAIN_HUMAN	Kallistatin	SQILEGLGFN#LTELSESDVHR
67	P35542|SAA4_HUMAN	Serum amyloid A-4 protein	LFGN#SSTVLEDSK
68	P53396|ACLY_HUMAN	ATP-citrate synthase	ILIIGGSIAN#FTNVAATFK
69	P60174|TPIS_HUMAN	Triosephosphate isomerase	SN#VSDAVAQSTR
70	Q14624|ITIH4_HUMAN	Inter-alpha-trypsin inhibitor heavy chain H4	LPTQN#ITFQTESSVAEQEAEFQSPK
71	Q8WVE0|N6MT2_HUMAN	N(6)-adenine-specific DNA methyl-transferase 2	EN#FSIYIFEYDK
72	Q08999|RBL2_H	Retinoblastoma-like protein 2	GKEEN#LTGFLEPGNFGESFKAINK

	UMAN		
73	Q96PD5|PGRP2_HUMAN	N-acetylmuramoyl-L-alanine amidase	SLN#ATELDPCPLSPELLGLTK
74	Q96N67|DOCK7_HUMAN	Dedicator of cyto-kinesis protein 7	KYLPVGCVTFQN#ISSNVLEESAVSDDV
75	Q4G0N4|CE033_HUMAN	NAD kinase domain-containing protein 1	QGN#LSLPLNR
76	Q06033|ITIH3_HUMAN	Inter-alpha-trypsin inhibitor heavy chain H3	KNAHGEEKEN # LTAR
77	Q6N021|TET2_HUMAN	Protein TET2	LQN#GSPLPER
78	Q6MZM0|HPHL1_HUMAN	Hephaestin-like protein 1	VFNEN#ESWYLDDNIK
79	P22792|CPN2_HUMAN	Carboxypeptidase N subunit	AFGSNPN#LTK
80	P09871|C1S_HUMAN	Complement C1s subcomponent	N#GSWVNEVLGPELPK